DOI: 10.13009/EUCASS2019-663

A New Design of an Embedded System for Online Harness Monitoring in Reusable Launch Vehicles Using Reflectometry

Nicolas Grégis, Mickaël Cartron* and David Monchaux***
**CEA, LIST, 91191 Gif-sur-Yvette, France*
nicolas.gregis@cea.fr, mickael.cartron@cea.fr
***CNES, 75012 Paris, France*
david.monchaux@cnes.fr

Abstract

The economical relevance of Reusable Launch Vehicles (RLV) highly depends on the Maintenance, Repair and Overhaul (MRO) costs, which should be kept as low as possible. For that purpose, providing efficient solutions for assessing the health state of a launcher is a crucial matter. This work aims at proposing a new paradigm for the assessment of the health of wires inside a launcher. After a description of the big picture of such a supervision system, its viability is examined in detail, considering all mission constraints.

1. Introduction

The philosophy of space programs has radically changed since its beginning. The development of commercial uses and the modification of the economic environment have led to rethinking reliability of launch vehicles as well as the cost-effectiveness of the whole chain of production [1]. It is nowadays necessary to take into account from the first concept study, and all along the conception, the entire life-cycle of the concerned systems. The main idea behind the RLV paradigm is to lower the cost/payload ratio with the help of reusability. If we consider Cd the project design cost, Cb the launcher build cost, Cmro, the Maintenance, Repair and Overhaul (MRO) cost, Nl, the number of launchers built in the program and Nf the number of flight per launcher, the total cost per mission Cm can be expressed as :

$$Cm = \frac{Cd}{Nl \cdot Nf} + \frac{Cb}{Nf} + Cmro \quad \textbf{(1)}$$

For a single-mission launch vehicles, Nf = 1 and Cmro is low. In comparison, the RLV concept is economically interesting only if Nf tends to be high and Cmro is kept as low as possible. For that reason, an efficient maintenance is a key factor to the economic success of such projects, and new tools and processes for maintenance and inflight equipment monitoring are needed. In the same time, Nf can be extended only if reliability is high.
During a mission, launchers are subject to very severe environments. Next to the engine, the temperature rises a lot in a limited period of time, and at the same time, the temperature goes low next to the tanks due to cryogenic environment. There are a lot of vibrations and acceleration is high. Among all launcher systems, the harnesses are particularly exposed to the stress induced by this environment. Temperature variations cause dilatation, which can lead to permanent breakdowns. Vibrations due to acceleration can cause short disconnections around connectors, these transients may be extremely short (a couple of microseconds) and impossible to detect once the launcher is at bay, but strong enough to perturb or stop the mission. It has been shown in [2] that a vast number of faults occurring in aircrafts happen during flight operations because of flight conditions. Mechanical stress can also alter the dielectric part of wires, which can quickly erode in a phenomenon called chafing, leading to short-circuit risks. In addition, temperature cycling causes significant stress on the dielectric of wires, reducing their performance and reliability.

DOI: 10.13009/EUCASS2019-663

There are several maintenance options to counteract the risks of breakdowns due to wires. A first option would be a systematic complete harness replacement, which does not require any previous analysis of any structural weakness. However, the cost of this option is high because it requires disassembly, reassembly and functional checking. Another possibility could be to keep the same harness between missions. The health of the harness could be estimated by a combination of visual and functional checks. However, without disassembly, visual checking cannot be exhaustive and it could be a delicate task, especially in compact launchers. Another option would be to provide an offline monitoring of the health of harnesses, any solution that would provide such a functionality could be designed so that wires are kept in place and could be useful for researching permanent damages. Finally, an online harness monitoring would also provide the ability to monitor the harness during flights, searching for intermittent faults in addition to permanent damages. In this last solution the monitoring system becomes a full part of the launcher, the monitoring is permanent, and every equipment could stay in place.
In this paper, we propose a solution that implements online and offline monitoring of harnesses, by the mean of reflectometry. This technique, which consists in analyzing electromagnetic wave propagation in a medium, has been successfully used in the field of cable diagnosis for many years. This method achieves a high precision in detecting and locating small defects and rapid transients, is non-destructive, and is easily configurable. To some extent, the reflectometry signal can be forged in order to fit some Electro-Magnetic Compatibility (EMC) pattern. Therefore, it is a great candidate to cover the objective of assessing health of harnesses. Some previous work has been done in aeronautics to make this technology available for on-line monitoring and it could also be beneficial to aerospace industry.
The paper is organized as follows. First, the reflectometry technique is presented. Then, details on the environment and harness configuration are given. After that, we will describe the faults that we aim to detect and locate, which will help quantify the requirements of the application. Then, the general organization of the monitoring system will be presented with a focus on the most critical aspects of the system, which could affect the feasibility of this concept. Finally, the concept will be validated after having verified the achievable performance, with the help of an analysis of the digital system on the one hand and with the help of a simulation on the other hand.

2. Reflectometry

Reflectometry is the study of reflecting waves in a medium. It is used in a wide range of fields such as acoustics, optics or electromagnetism. For example, a well-known application is radar measurements in aeronautics, but ultrasound for medical purpose is also a derivative of the theory of reflectometry.
The base principle is the following: a wave is generated by a reflectometer at a specific location of the medium and it propagates through the medium. Any singularity in the medium redirects the wave and its energy into multiple directions. The reflectometer has also a sensor that captures the global response of the medium to the energy introduced into the medium. The state of the medium is established by analyzing this global response. For example, an echo during a radar detection indicates the presence of an obstacle for the electromagnetic wave traveling in free space, and moreover, the delay between the instant of generation of the incident signal and the reception of the reflected one carries the information of the distance between the detected object and the observer.
Reflectometry in wire diagnosis has been used almost since the creation of electromagnetism as a field of physics, mostly for the purpose of detecting a severe cut in a line, but its generalization to complex systems via embedded electronic sensors is recent [3], [4]. When the medium is a combination of two wires, the wave propagation is limited to one dimension and the nature of the wave which propagates is the combination of voltage and current. We call the wire system the Network Under Test (NUT). Figure 1 illustrates a reflectometer monitoring a simple wire network.

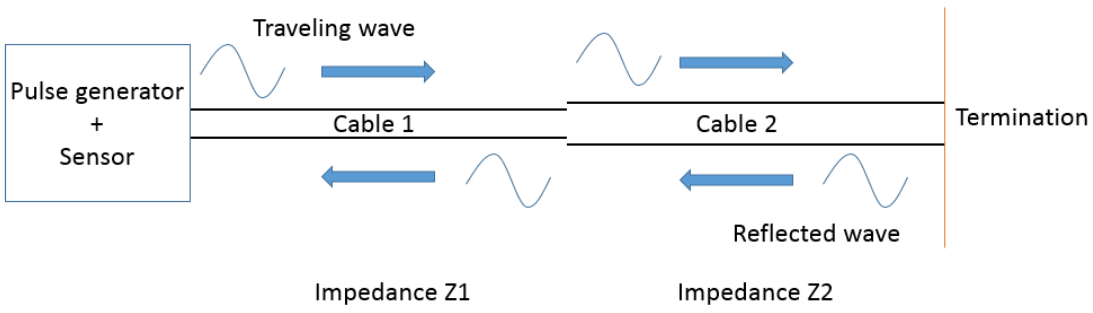

Figure 1 - principle of cable diagnosis via reflectometry

In the case of complex networks, such as ones presenting several junctions, or combining different sets of devices, the resulting response is complex and its analysis becomes challenging. Each ramification of the network generates an ambiguity in the interpretation of echoes, and equipment may act as filters for the traveling wave, reducing the tested

DOI: 10.13009/EUCASS2019-663

area or making it completely unreachable. The introduction of several sensors, plugged at different extremities of such a network can be used to suppress ambiguities [5]. This approach, as well as others [6] [7], enables the development of embedded solutions based on microelectronic devices for online diagnosis. Such solutions have been successfully used in a large variety of fields, from automotive systems [8] to aircrafts maintenance [9]. The progress of microelectronic components, combined with new signal processing methods, gives today the possibility to reach higher levels of performance and thus detect smaller defects.

3. Description of the specific environment of RLV for reflectometry usage

Within the frame of project CALLISTO [10], a monitoring system for harness diagnosis has been considered. It is important to detail the environment in which it will be deployed and the constraints it can generate for the dimensioning of the solution.

First of all, a RLV possesses many types of cables: some are used for connecting antennas to communication systems, other to carry power, some transport command signals to mechanical parts, and so on. All these types of cable are subject to deterioration over time and present a malfunction, which can hinder flight operations. However, some are more critical than others and the gain of adding sensors is not evident for all. Actually, adding sensors makes sense for complex topologies and for cables that are hard to access. Thus, in the case of CALLISTO project, cables carrying power from batteries to RLV's organs have been chosen to demonstrate the performances of the reflectometry system. They are among the critical ones because they power all important organs of the vehicle, are installed throughout its structure, and they form a complex topology, making them the best candidates for monitoring demonstration. In addition, the low frequency currents they carry is easily manageable for a reflectometry sensor, in order to assure complete harmlessness on the system.
These cables are mainly bifilar transmission lines made of copper and polyethylene. Various models can be found in literature and they do not necessitate a complex modeling for simulation purpose. There are 3 types of cable lengths given in the scope of CALLISTO: 10.10 m for connecting both ends of the structure, 1.05 m between distributors and switches and 0.7 to 2.76 m for cable connected to RLV organs. The typical topology encountered is presented in Figure 2.

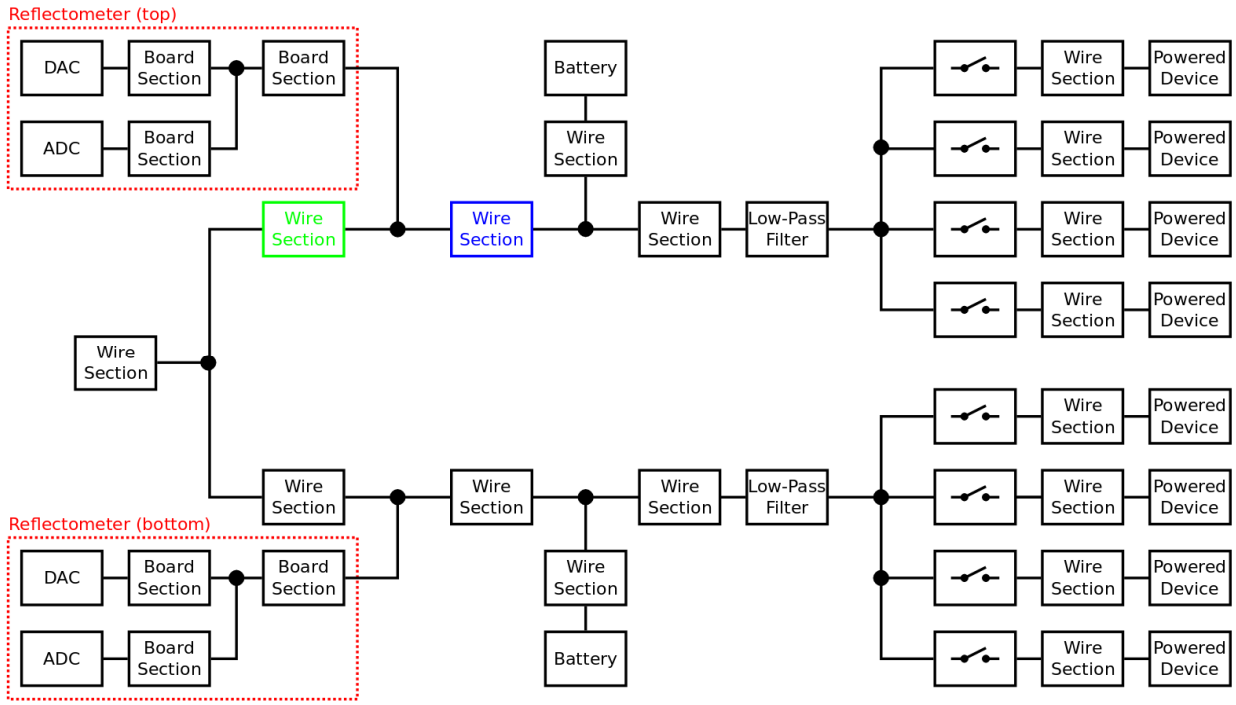

Figure 2 - Topology used for simulation

Reflectometry sensors would be installed at strategic location on the cable network in order to maximize the coverage done with reflectometry. It means that they need to be connected through specific connectors on the cable and powered up as any other equipment of the RLV. The best possibility is to have the sensors installed near the power distribution boxes at both ends of the vehicle. It reduces the additional cables used for in-between sensors and power supply and it is a key position in the network in terms of coverage.

DOI: 10.13009/EUCASS2019-663

The complexity of the power network is not only the consequence of its topology, but also the consequence of the number of equipments connected to it, as seen on Figure 2. Every element may represent an obstacle for reflectometry analysis.
Batteries are complex electrical systems, which generate additional reflections on a reflectometry measure. Literature gives us some models for them [11] and as a first approach, these models are sufficient to integrate them in the simulation process described in later chapter.
The filter cited on Figure 2 is supposed in our project to be a simple low pass filter with a cutoff frequency of 1kHz. The loads, representing the RLV components are highly dependent of the technological choices made for the RLV and can't be known at this stage of the project, however, with the presence of the low-pass filter, it may be assumed that they have a limited impact on the reflectometry measures.

4. Defect modelling

During flights, harnesses are exposed to severe environmental conditions, like high levels of vibration, chemical aggression, radiation, or temperature cycling. Each of these event types could leave a trace on reflectometry measure, and deserves a consideration. However, in the scope of the feasibility demonstration for CALLISTO, there are still too many unknowns to correctly treat all possible cases.
Vibration-induced chafing would be one of the most critical type of degradation. Cables affected by it may remain operational for a long time, as long as their internal conductor is not affected, but as time passes, the coating over the conductor is removed and there is a growing possibility of a physical connection between two conductors. When this happens, it generates a short-circuit, which can have dramatic consequences. With the vibrations still present, the contact between the cables becomes intermittent and can repeat many times during flight operations. Such degradation and the consequences it has is the first type of defect our monitoring system aims to detect and localize.
From a reflectometry point of view, this type of defect is a hard fault, meaning a total reflection of propagating signals on the position of the defect. A sensor installed at one side of this defect will see the network as if it had been cut in half, all points after the defect becoming unreachable. The principle of the reflectometry approach is presented in Figure 3. The detection difficulty lies on the duration of the defect and its position in the network. Multiple reflections and attenuation can mask an important fault.

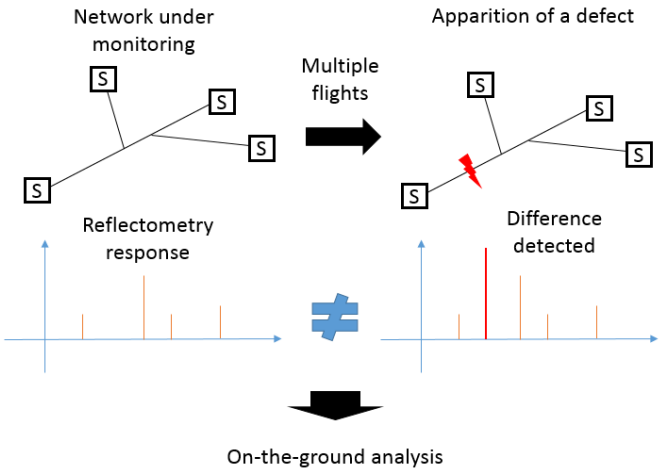

Figure 3 - Principle of the detection of a hard fault on a harness by a reflectometry system

Chemical aggressions and radiations are secondary to temperature cycling, which has a far more direct impact on wave propagation conditions and which is more prominent to appear. Indeed, during flight operations, RLVs operate in an environment where temperature varies between ground temperatures to very low temperatures in high altitude. Furthermore, cables, in addition to experiencing the same variations, may be installed near the propellant tank, which temperature reaches extreme cold, or near the rocket engine where temperature rises considerably. Even though propellant is isolated with thermal protections, the ambient temperature can be affected. In particular, a defect in the protections could mean a frozen spot on the cables, and thus a local degradation.
From this reasoning, two aspects of thermal cycling emerge: the possibility of small local degradations due to extreme cold and the progressive effect of global temperature changes. In the first case, it is the polyethylene coating of the cables whose electrical properties are modified. The carbonated structure undergoes irreversible structural changes which will progressively be the source of a new defect. From a reflectometry point of view, the local changes of electrical properties induce a change in characteristic impedance and thus a reflection of propagating signals.

DOI: 10.13009/EUCASS2019-663

In the second case, the polyethylene structure is impacted, but the electrical properties of the copper conductor are also modified on a scale large enough to have an impact on reflectometry measures. If the temperature is homogenous along the cable length, it will not induce any local reflection, but rather a change in attenuation of the cable and wave velocity of traveling signals.
To model these two effects, it is possible to work on the propagation model used for cables. The classical description used for wave propagation comes from a model called “the telegraphists’ equations”, which describes a cable as the chaining of infinitely small cells of electrical components R, L, C and G. Dependence of these parameters with temperature is well documented in literature [12] and it allows us to model the impact of both scenarios by means of RLCG modifications. In the first case, the modification is concentrated on a small part of the cable and corresponds to a drastic drop of temperature, and in the second case, the modification is applied to the whole length of the network, or a part of the network, and corresponds to a various range of temperature encountered during flight operations.

5. System organization

CEA List proposes a new architecture combining its knowledge on reflectometry and system integration to respond to both objectives and listed constraints. It is divided in two parts:

- an external software which is installed on the ground and is responsible for data processing and human to machine interface,
- embedded sensors connected to the harness of a RLV or a demonstrator like CALLISTO.

The external software in itself is made to run on a classical computer, or similar device, best suited for use by a technician. It is mainly composed of a specific interface, which allows a setting of the sensors once the two parts are connected. But since it establishes a virtual link to the sensors, via a communication protocol carried over Universal Serial Bus (USB), it is also the medium over which measured data is repatriated after flight operations. A database stores all measures and can be interrogated to retrieve previous information. The last part of this software contains specific post-processing algorithms used on demand on data to detect the presence of any defect and its position on the harness.

The sensors, designed for CALLISTO project, are a complex combination of a FPGA, a microcontroller and external processing components, such as numeric correlators or memory blocks. Each sensor has the capacity to generate reflectometry signals thanks to the analog-to-digital convertors of its FGPA, and to make a pre-processing of the data through the usage of its microcontroller. This element also drives all in-and-out communications. Memory is used to store measurements for the duration of the flight.

Figure 4 presents the interaction between the two parts of the system and all the elements of its environment.

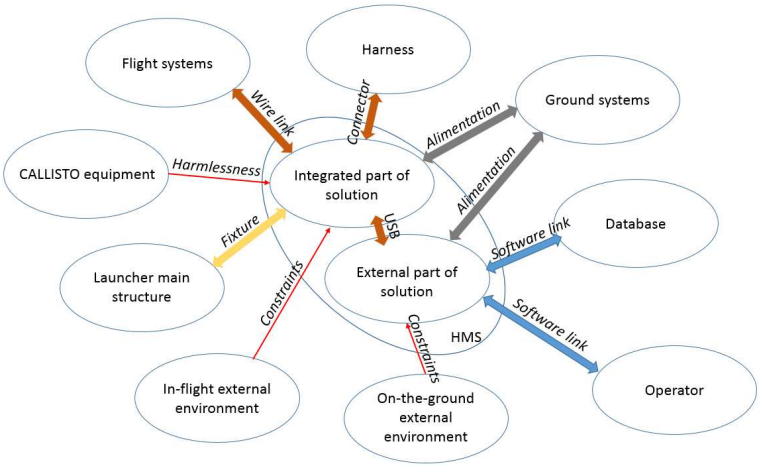

Figure 4 - Interaction of sub-parts of the system with its environment

This analysis shows the constraints such a choice imposes on the system and also some of the proposed solutions compatible with this type of architecture. One of the main advantages of electronic boards is their reduced volume and their low energy consumption. However, as we can see, the choice made here generates the need for a high number of connections between elements, either physical or digital. To limit their number, and the cost they generate, it has been chosen to proceed with master/slave architecture. It means that, for demonstrator like CALLISTO, there is a sensor

DOI: 10.13009/EUCASS2019-663

assuming the role of master. It is the only interface between the software part of the solution and the mesh of sensors installed in the launcher. It then communicates to all other sensors through a unique link and serves as the gateway to the processing software at the time of data repatriation.
During flights, sensors are powered by the launcher's battery, and during maintenance through the link connected to the master. Such a choice of architecture allows to fully benefit of the RLV's life cycle. The connections are limited to their minimum during flight operations, and in maintenance phases, an operator could easily access all sensors settings or measures directly through the software interface connected to the master sensor.

6. System operation

The system operation depends on the life cycle's phase. Table 1 presents the different life cycle's phases and the objective of the cable monitoring system for each phase. Since the RLV is used for several missions, phases 2 to 5 occur on a loop.

Table 1 - Objectives and access to RLV during life-cycle

Phase	**1 Installation in RLV**	**2 Pre-flight phase with total access**	**3 Pre-flight phase with limited access**	**4 Flight operations**	**5 Maintenance phase**
Objective	Sensor test	Sensor set-up (calibration, reference measurements)	Defect monitoring	Defect monitoring	Defect monitoring / data analysis
Access to sensors	Full	Full	None	None	Full

Typically, an operator using the system would install it at the beginning of a flight campaign, tests it, set the right parameters according to regulation. Then, the RLV would be transported to the flight area, disconnected from all links to the ground, take off and come back after its mission. Once the links to the ground are disconnected, the sensors would switch to an autonomous mode and start sending reflectometry signals and recording events. All data would be extracted during maintenance phases.
As previously detailed in section 4, the system must track very quick intermittent defects, as well as slow degradation phenomenons. To address both issues, the system switches between two monitoring modes. The first mode is called *intermittent defect search mode*. In this mode, the different sensors alternatively take possession of the medium by the mean of a token sharing. When holding the token, a sensor performs one measurement with a configuration of parameters optimized for the acquisition speed, record it, and adds a timestamp to it and release the token. Every capture is compared to a reference capture, and if there is enough difference between them, with respect to a configurable threshold, this constitutes the beginning of a detection event burst. Several capture before and after this first detection are done, stored, and timestamped. In order to make the difference between an intermittent defect and slow variations phenomenons, the reference capture is regularly updated at a configurable frequency by taking a fresh capture. The reference capture is realized with the same configuration of parameters, so that references and instant capture are fully comparable, and all reference captures are also timestamped and in addition they are stored in memory for the whole flight.
The second measurement mode, called *slow degradation search mode*, allows to address the problematic of progressive degradation. At a given frequency, the system switches from the intermittent defect search mode to slow degradation search mode. In this new mode, the sensor is reconfigured in order to produce a higher resolution reflectogram, which is recorded and timestamped. Immediately after that, the sensor returns to intermittent defect search mode, to limit as much as possible the fault coverage degradation of intermittent defects.
At ground, all generated data is downloaded in order to proceed to its analysis. Then, the data analysis is done off-line, by estimating key parameters, like wave velocity or characteristic impedance, for example. The timestamps associated to captures are used to do some temporal correlations with other sensors, such as accelerometers or temperature sensors, which already exists in other devices in the launcher.

Now that the general scope of the system is given, there are questions about the feasibility of such a monitoring system. The time constraints on the switching between the two modes is important as it generates blind time slots in which information is lost. The systems should be implemented on a space-grade FPGA, with limited resources. The following chapters focus on the feasibility analysis.

DOI: 10.13009/EUCASS2019-663

7. Feasibility analysis

7.1. Description of the system

In terms of components, the reflectometry architecture is made of:

- a DAC, which produces an excitation signal which is injected in the cable network under test. This component has a resolution of *rdac*.
- an ADC, which is used for capturing the response of the cable network under test. Its resolution is *radc*.
- an FPGA, which drives the DAC and ADC.

The first step of a reflectometry capture consists in producing a generation signal. This generation signal is noted *S*. This signal is periodic, made of *n_sig* samples updated at a *fdac* rate. The period of *S* is *n_sig/fdac*.
The signal at the input of the ADC is noted *R*, for response. It is a modified version of *S*, which was passed in a filter which reflects the effects of:

- the cable network under test,
- other contributions due to the electronic board itself.

R is also a periodic signal like *S*, with the same period *n_sig/fdac*. The aim of the signal acquisition part is to provide a discrete version of *R*, sampled at a *facq* frequency; the discrete version of *R* is noted *R'*. The ratio *facq/fdac* is an integer and is noted *sacq*. In order to provide a high *facq* value while working with a simple hardware, the acquisition is done in several passes, (*sph*) passes, made of *nsig*sacq/sph* samples each, and each pass being done with a different phase.

$$sph = nchan \cdot sacq \tag{2}$$

All phases are equally distributed with a step of *360°/sph*. Between every phase pass, the acquisition is paused until the ADC clock is reconfigured and stabilized, which is done in *tpllreconfig* (time).
In order to filter potential noise, all *sph* phase captures are performed *avg* times each. Then, the *avg* complete acquisitions are used to produce an averaged acquisition made of *sph* vectors of *nsig*sacq/sph* samples each. The vectors are noted B_p with $p \in [1, s\_phase]$.
Most of the reflectometry analysis is based on the analysis of reflectograms. A reflectogram is the result of the intercorrelation between the generation signal and the response signal. There are three steps to follow in order to get a reflectogram from the averaged phase vectors. The first step is called pre-interleaving. It consists in presenting the data in a specific format so that the intercorrelator can process them. The data enters the pre-interleaver in the form of *sph* vectors B_p of *nsig*sacq/sph* samples, and it is outputted in the form of *sacq* vectors of *nsig* samples. This output vectors are noted C_q with $q \in [1, sacq]$. Then, the intercorrelator processes *sacq* times an intercorrelation of *S* and C_q, which produces *s_acq* different output vectors of size *nsig*. These output vectors are noted D_q with $q \in [1, sacq]$. Finally, a third module called post-interleaver is in charge of transforming the D_q vectors into a single vector of size *nsig * sacq*, by interleaving the samples of all D_q vectors. We note *E* the resulting vector, and we call it the instant reflectogram.
The detection of an intermittent fault consists in comparing the instant reflectogram *E* with a previously acquired reflectogram. This comparison is done by a module named *detector*. This module take for inputs: a- the reflectogram E, b- another previously acquired reflectogram (the reference reflectogram) noted *Ref*, and c- a threshold vector noted *T*. All three input vectors are the same size. The detector provides three outputs:

- a Boolean indicating the detection status,
- the position of the maximum of $|E - Ref|$ where $|E - Ref| > T$,
- the value of the maximum of $|E - Ref|$ where $|E - Ref| > T$.

The reflectogram *E* is also written to memory by a module named *DMA*, which stands for Direct Memory Access.

7.2. Dimensioning the system

The performance of the reflectometry system declines in several aspects. First, the *maximum network size viewable* is noted *Lmax*. The signal must be able to propagate to the most remote place of the network and to propagate back to the injection point, in a time lower than the period of the reflectometry signal. If this condition was not met, it would mean that the repetitive signal would loop so quickly that the direct propagation effects would not be visible in the first order reflectogram. We define *Lmax* as:

DOI: 10.13009/EUCASS2019-663

$$Lmax = \frac{c \cdot cp \cdot nsig}{2 \cdot fdac} \quad \textbf{(3)}$$

The **reflectogram spatial resolution** Res_s is the distance step between two reflectogram samples. It is desirable to have a low Res_s value compared to the typical distances at stake in the network. It is expressed as:

$$res = \frac{c \cdot cp}{2 \cdot sacq \cdot fdac} \quad \textbf{(4)}$$

The **bandwidth** of the reflectometry signal is an important performance view. From a bandwidth point of view, two defects too close from each other would appear as a single lobe, so the ability to discriminate two defects located in the same area is efficiently described by the bandwidth. Since the reflectometry signal is periodic and discrete, the frequency specter is discrete and has the shape of a cardinal sine. Theoretically, for a temporal signal of frequency sample *fdac*, the norm of the corresponding frequency specter has zero-crossings at frequencies $i \cdot fdac$, with *i*, a positive number. We define the reflectometry bandwidth as the bandwidth formed by the first order lobe of the cardinal sine. In our case, the bandwidth spans in $[0, fdac]$.

The **minimum time of an intermittent defect** is defined as the minimum duration of a defect, so that the system cannot miss it. In order to estimate the value of this performance criteria, it is necessary to go deeper into system performance considerations. Figure 5 illustrates the sequence of the reflectometry supervision when searching for intermittent faults. The reflectometry capture is an active measurement, that means that the sensor needs to send an excitation signal on the network prior to sensing. In our case, the network is made of several (*nmod*) reflectometry sensors that need to share the same medium. The technique that was chosen for medium sharing is TDMA (Time-Division Multiple Access), which means that the various sensors are granted the network one at a time. The sharing is realized by implementing a token-based protocol: there is a unique token, and a sensor is allowed to generate some signal on the network when it has got the token. On Figure 5, nmod = 2, and the token is first given to A, then to B, and then to A again. During the time a sensor is waiting for the token, its reconfigures itself to be ready when it gets the token back. When a sensor obtains the token:

- it begins generating some signal for a certain period of time without acquiring anything,
- then, it proceeds to *avg* acquisitions of *n_ph* phases, separated by phase reconfiguration periods.

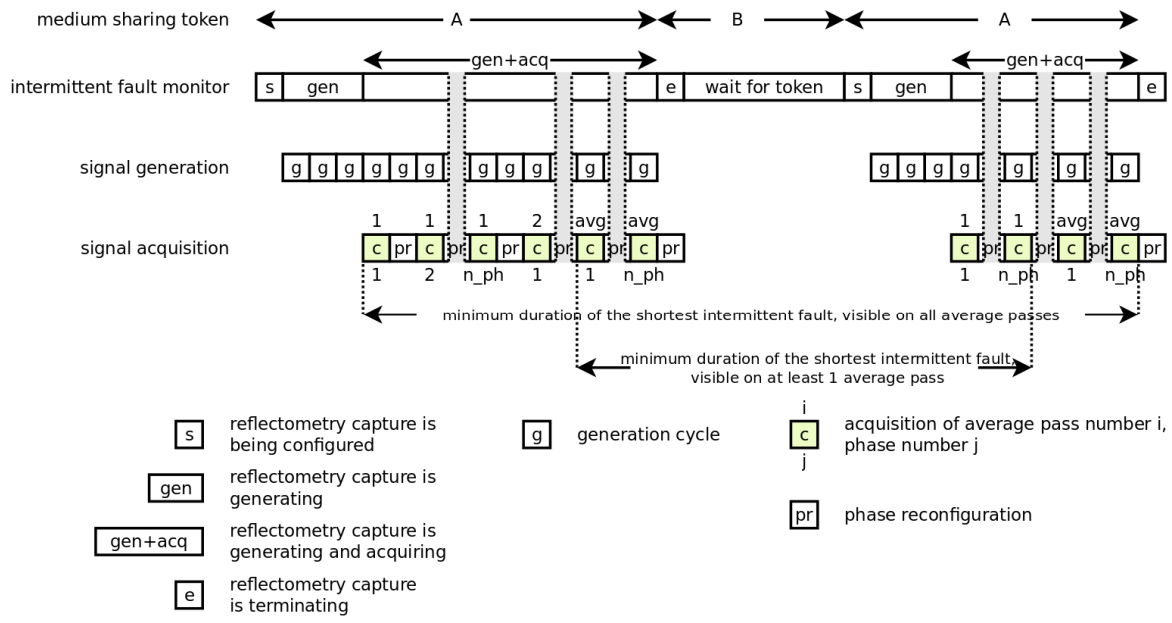

Figure 5 - Sequence analysis for establishing the worst case minimum duration of the shortest fault for all average passes or just one average pass

The sensor is “blind” during several instants and it actually senses the networks during the moments colored in green. Figure 5 exhibits the worst case situations for establishing:

- *FDAP (Fast Defect All average Passes)*: the minimum duration that an intermittent fault must have so that it appears on all complete average passes,

DOI: 10.13009/EUCASS2019-663

- *FD1P (Fast Defect 1 average Pass)*: the minimum duration that an intermittent fault must have so that it appears on at least one complete average pass.

$$FDAP \geq tWaitForToken + tst + 2 \cdot nchan \cdot sacq \cdot tpc \quad \textbf{(5)}$$
$$FD1P \geq tWaitForToken + tst + 2 \cdot nchan \cdot tpc \quad \textbf{(6)}$$

In this expression:

- tst is the time spent while generating, waiting for the permanent state to establish: $tst = \frac{nst \cdot nsig}{fdac}$, with $nst = \frac{2^{\left\lceil log2\left(\frac{2 \cdot nrt \cdot fdac \cdot ltyp}{c \cdot cp}\right)\right\rceil}}{nsig}$,
  - tpc is the time spent for capturing one phase, plus the associated phase reconfiguration time: $tpc = \frac{nsig}{fdac} + tpr$,
  - tWaitForToken is the time spent waiting for the token: $tWaitForToken = (nmod - 1) \cdot (tst + avg \cdot nchan.tpc)$.

Studying the feasibility on reflectometry on a spatial mission means considering the computation target. Yet, space-grade FPGA are globally more expensive and offer less resources than their commercial- or industrial-grade counterparts. For that purpose, apart from strictly performance-oriented criteria, the resource usage of the FPGA should be checked.
The first kind of resource evaluated is the quantity of required memory blocs. We suppose that a typical space-grade FPGA memory block can store either 512 9-bit words, 256 18-bit words or one double clock FIFO.
The elements requiring memory blocks are summarized in table 2.

Table 2 - List of elements requiring memory blocks

Element to store	Number of items	Width of items (bits)	Number of memory blocks required $\left\lceil \frac{numberOfItems \cdot width}{9 \cdot 512} \right\rceil$
S	$nsig \cdot sacq$	9	$\left\lceil \frac{nsig \cdot sacq \cdot 9}{4608} \right\rceil$
FFT(S)	$2 \cdot nsig \cdot sacq$	18	$\left\lceil \frac{2 \cdot nsig \cdot sacq \cdot 18}{4608} \right\rceil$
Ref	$nsig \cdot sacq$	18	$\left\lceil \frac{nsig \cdot sacq \cdot 18}{4608} \right\rceil$
T	$nsig \cdot sacq$	8	$\left\lceil \frac{nsig \cdot sacq \cdot 8}{4608} \right\rceil$
Work memory dedicated to avg block	$2 \cdot nsig \cdot sacq$	18	$\left\lceil \frac{2 \cdot nsig \cdot sacq \cdot 18}{4608} \right\rceil$
Work memory dedicated to pre-interleaver block	$2 \cdot nsig \cdot sacq$	18	$\left\lceil \frac{2 \cdot nsig \cdot sacq \cdot 18}{4608} \right\rceil$
Work memory dedicated to post-interleaver block	$2 \cdot nsig \cdot sacq$	18	$\left\lceil \frac{2 \cdot nsig \cdot sacq \cdot 18}{4608} \right\rceil$
Storage of intermittent defect burst of size highSpeedPlaces	$highSpeedPlaces \cdot nsig \cdot sacq$	18	$\left\lceil \frac{highSpeedPlaces \cdot nsig \cdot sacq \cdot 18}{4608} \right\rceil$
Storage of a single high resolution capture	$nsig \cdot sacq$	18	$\left\lceil \frac{nsig \cdot sacq \cdot 18}{4608} \right\rceil$
2 double-clock FIFOs for domain transition			2

The evaluation of logical/register resources is a difficult process. This study does not yet cover this aspect. However, several solution can help maintain low the usage of logical and register resources. The intercorrelator is the main user of logical and register resources. The complexity of this module only depends on the size of the intercorrelation, which is *nsig*. This intercorrelator is not compulsory when acquiring a high resolution reflectogram, but only for high speed reflectograms, which precisely use a lower value for *nsig*. A complete evaluation is extremely difficult to do without producing the code and using the FPGA tools. This is beyond the scope of this study and will be examined in the future.

DOI: 10.13009/EUCASS2019-663

8. Simulation method

For this work, we tested the elements of previous chapter, thanks to a simulation tool created by CEA List. This chapter will detail the core mechanisms of this method and the necessary hypotheses for simulating all types of defects selected in the project CALLISTO.

8.1. Mechanisms of the simulation method

The simulation tool which was used in this work is a frequency-based electrical simulator. It includes modules for modeling cables, analog parts, junctions, and digital processing. As explained earlier, the RLV context imposes a limited choice upon the selection of useable components, and as explained in previous chapter, the key parameters that are spatial resolution and time resolution are dependent of the choices made for each step of the digitalization process, both in emission and reception.
The first step of the modeling is the definition of the signal used by the reflectometry system. In this case, it is a simple square pulse for TDR. But since it is generated by DAC of the FPGA, in addition the shape of the signal, the characteristic of the DAC becomes also a variable in the simulation. It is set using the results presented in chapter 6. At this point, the generation of the signal is covered, but the acquisition must also be added in the simulation to account for the quality of ADC of the FPGA. In particular, the number of acquisitions in a measure as well as the oversampling factor are integrated as variables. To complete the digital part of the sensors, a non-perfect model of the correlator is also considered.

The analogical part consists in the addition of all the elements present in the path of the propagating signal that may generate losses or reflections. They are the following:

- Cables of the harness. Their nature, as well as the topology, is central in the simulation. Their model is precisely detailed in terms of electromagnetic elements on which the characterization of defects is based.
- Battery used for alimentation of the RLV. The monitored cables are connected to them and their presence generates reflections and modifications of the propagating signal.
- Analogical filters used to separate low and high frequency signals before powering components of the RLV.
- Switches used to command the usage of component of the RLV.
- Components powered by the battery.
- The other reflectometry sensors present on the network.

Once every element is associated with a propagation model, they are assembled, following the structure of the monitored launcher and a reflectometry measure can be synthetized through a numerical calculus. In presence of a defect or a modification of one element, the concerned model is changed and the simulation result is generated again. A comparison between the two results is then processed to emphasize the effect of the defect and conclude on the feasibility of reasonable detection and localization.

8.2. Simulation settings

Several sets of simulations have been generated following this principle. The first set was made to test the possibility to detect hard faults at different positions in the monitored network. The reference reflectograms seen by each sensor were simulated and then the network was redefined to correspond to a configuration with fault, then reflectograms were generated again. As said in chapter 3, an open circuit has been made in the wire section highlighted in blue.

The RLCG parameters of the cable were set to match bifilar lines of characteristic impedance of 110 Ω, the resistivity was that of copper at 20°C and with the permittivity of PVC.
For the digital part:
- resolution is set to 10 bits,
- maximum output current is set to 20 mA,
- saturation tension is 1.25V,
- non linear integral effects are considered,
- non linear differentiation effects are considered.

For the simulation of temperature effects, three scenarios were considered: a uniform temperature change on the cable, a local change of temperature over 15 cm of the cable and a local change of temperature over 1 m. The first one aims to simulate the impact of the environment on the measure during flight operations, the other two the presence of a local effect due to a fault in the cold thermal protection or overheating due to combustion. In each scenario, RLCG parameters of the cable were set for 6 temperature levels: 200 K, 250 K, 273 K, 293 K, 323 K and 373 K. This allows

DOI: 10.13009/EUCASS2019-663

to cover both extremely cold and hot temperature. Reflectograms were generated for each case. The defects were simulated on the wire section highlighted in green in Figure 2 of chapter 3.

9. Results

9.1. Resources evaluation

In this reusable launcher context, we consider the following environmental/host system parameters:

- cp = 0.7 . This is a typical propagation coefficient.
- Lmax ≥ 17m. The most remote points of the network are separated by approximately 17m.
- nrt = 4. At every reflection of the reflectometry signal, the signal loses a lot of energy. It is more relevant to count the number of reflections rather than counting the propagation distance, in order to estimate when the energy was absorbed in the network or has reached a permanent state. nrt = 4 means that after 4 round trips, the energy is entirely dissipated.
- nmod = 2.

Then, we suggest using these technological choices:

- Bandwidth : [0 Hz, 200MHz]. Which means that fdac = 200 MHz.
- nchan = fdac/fsys = 2. On the one hand, we aim fdac = 200MHz. On the other hand, the rest of the system is limited by the digital architecture. By experience, we know how to design reflectometry architectures that can be clocked at around 100 MHz. As a consequence, we consider nchan = 2.

Then, the application analysis provides two constraints:

- Res ≤ 15 cm : the minimum spatial resolution when capturing a high resolution reflectogram,
- LD1P ≤ 10µs. The shortest intermittent defects we want to detect are of the same order than pyrotechnical shocks, which are estimated around 10 µs.

Finally, the choice of a spatial-grade FPGA adds resource constraints:

- the number of memory blocks must be lower than 112, so that we can use already available FPGAs at a reasonable cost,
- the number of logic/register blocks must not exceed the available resources.

After having reduced that scenario into equations, all free parameters can be estimated. According to equation (4), there is a direct relationship between the oversampling factor sacq and the spatial resolution res. Figure 6 shows the resolution as a function of sacq. According to this figure, sacq should be configured to 4 for high resolution reflectograms, in order to reach the requirement of 15 mm for res. For high speed capture, we consider that sacq could be reduced at 2, if necessary.

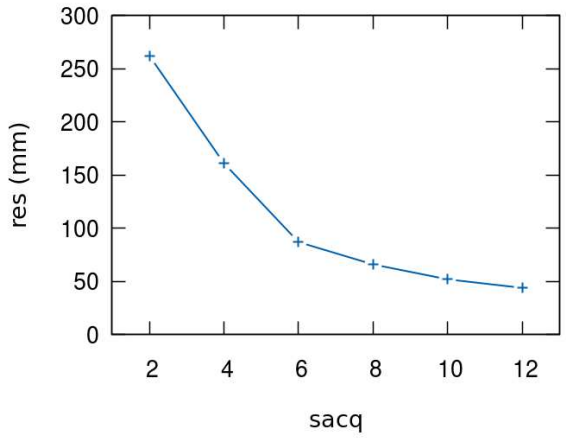

Figure 6 – Resolution res as a function of sacq, the oversampling factor

Now, there is a direct relationship between the nsig parameter and Lmax (c.f. equation (3)), and Figure 7 illustrates this relationship. The required Lmax can theoretically be achieved starting from nsig = 64. That is the ideal tuning for

DOI: 10.13009/EUCASS2019-663

high speed captures. However, choosing a higher value would provide reflectograms with less multiple path effect, so we prefer using nsig = 512 for high resolution captures.

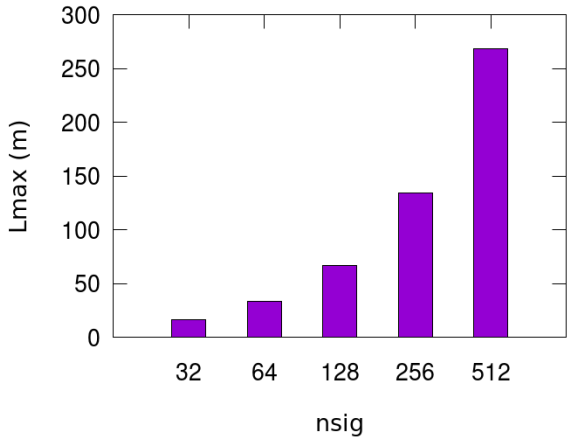

Figure 7 – Maximum distance of the reflectogram (Lmax), as a function of nsig

Equation (6) expresses the fastest visible defect as a function of many parameters. Among them, the parameter tpr represents the time needed to reconfigure the phase of the PLL between two phase captures. Considering the high speed capture configuration, we have to determine the required maximum PLL reconfiguration time so that the fastest visible defect duration is lower or equal to the application constraint of 10 µs. Figure 8 shows the LD1P parameter as a function of tpr, considering sacq = 2, and nsig = 64 (high speed configuration). According to this figure, the PLL must be able to reconfigure in a time lower or equal to 300 µs. More precisely, in this time budget, the PLL should reconfigure and the jitter of the clock and of all clocks below should be stabilized.

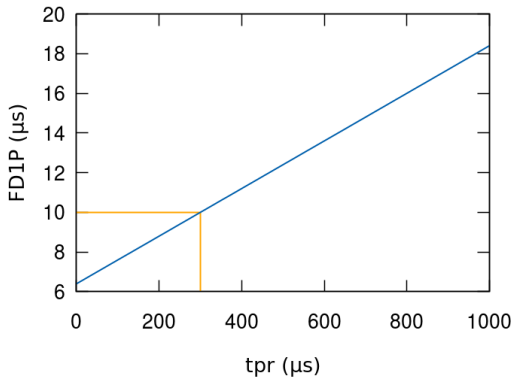

Figure 8 – Fastest duration of an intermittent defect as a function of tpr, the time for one phase reconfiguration.(sacq=2, nsig=64)

This reasoning raises a question: is it possible to fit this application, with the above requirements into a space-grade FPGA? To answer, let us consider the memory blocks first. The application will be able to realize both high resolution and high speed scenarios, but we consider the latter — which is the most constraining one — for memory usage considerations. According to Table 2, and considering sacq = 4, avg =16, and 8 places for storing intermittent fault sub-events and 1 place for storing a high resolution reflectogram, we get the result of Figure 9, which shows the number of required memory blocks as a function of nsig. With the FPGA considered as an example, that has 112 available memory blocks, nsig could have a maximum value of 512. Beyond that limit, a bigger FPGA would be required.

DOI: 10.13009/EUCASS2019-663

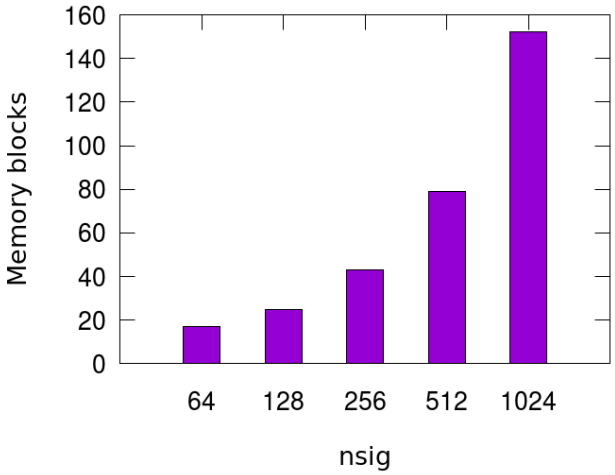

Figure 9 – Memory block usage for various values of nsig, (sacq=4, avg=16)

The evaluation of the logic/register blocks usage was also done by considering the high resolution scenario.

9.2. Intermittent fault detection

Let's have a look now at the results of the simulation of an intermittent fault. The considered fault is an open circuit that occurs in the middle of the wire section marked in blue in Figure 1. Figure 9 shows the differential reflectograms at top and bottom reflectometers obtained with the reflectometry simulator configured in high speed mode (nsig=64, sacq=2, fdac=200MHz). A differential reflectogram is the difference between the instant reflectogram (containing the intermittent fault) and the reference reflectogram. On this reflectogram, the maximum of the curve (in absolute value) corresponds to the distance to the defect we are searching for, which means that the system would correctly locate the fault.

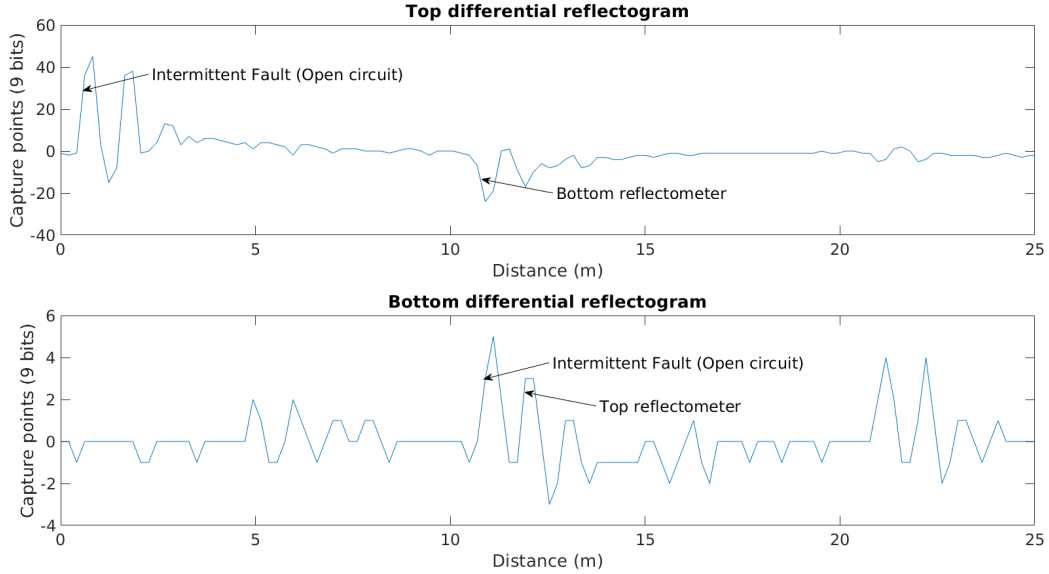

Figure 9 – Differential reflectograms when an open circuit suddenly happens, for top and bottom reflectometers

9.3. Detection of temperature effect

Results of the simulations of temperature effect, applied on the green wire section of Figure 2 are presented on Figure 10, Figure 11 and Figure 12. The figures shows the differential reflectogram between the reference measure and the ones for each temperature. As we can see, the temperature generates shifting of reflectograms due to celerity changes, but also new reflections all over the cable. However, in the case of the short defect (15 cm), it represents only a few points in the dynamic of measure, which is really close to nothing. It can be inferred that in real conditions, such a

DOI: 10.13009/EUCASS2019-663

defect will be masked by noise and other sources. For the two other cases, the number of points is enough to conclude that the defect can effectively be detected for all temperature levels.

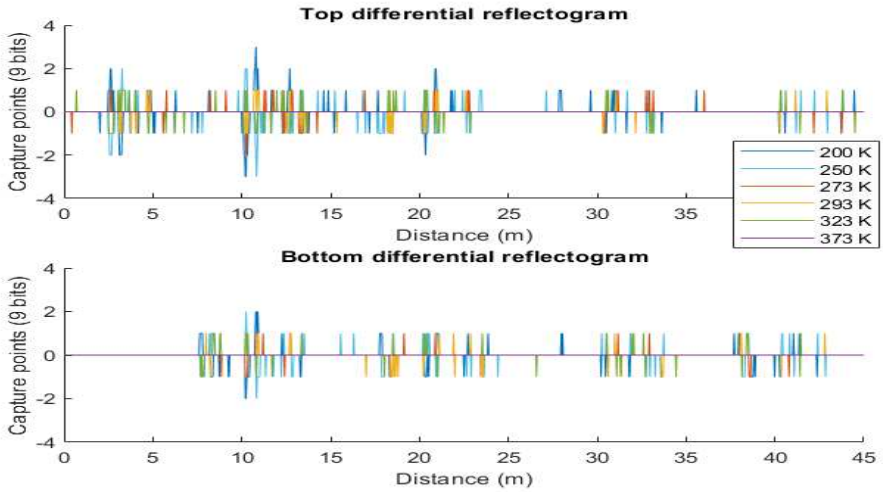

Figure 10 - Results of simulation for short temperature defect

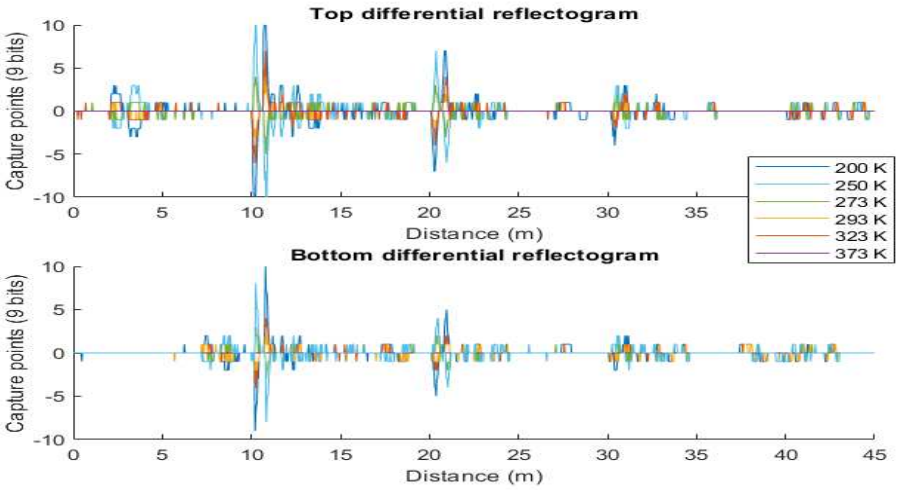

Figure 11 - Results of simulation for medium temperature defect

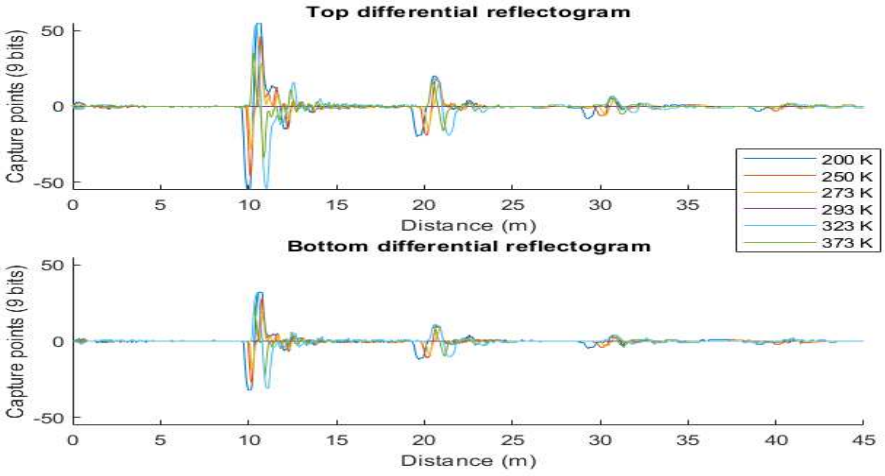

Figure 12 - Results of simulation for long temperature defect

DOI: 10.13009/EUCASS2019-663

10. Conclusion

During the realization of this work, a first system was designed, dedicated to the monitoring of fast intermittent devices and as well as slow degradation of defects in wires. Also, a realistic dimensioning of this system was proposed, which considers the constraints that come with RLV, in particular with a use of space-grade programmable devices. A simulator dedicated to the simulation of reflectometry systems and electrical networks was used to give estimated views of the reflectograms that the reflectometry modules could generate, considering the optimized parameters calculated in the preliminary dimensioning step. The analysis of this estimated data allows to conclude that the system is promising for detecting and locating very fast intermittent defects down to 10µs. For modifications due to temperatures typical of the intended mission, the reflectograms are precise enough to detect them, down to one-meter sections.
The interest of on-line and off-line health assessment of the health of wires for optimizing the maintenance, repair and operation costs is reinforced by this first study. However, we plan to go deeper into the feasibility assessment, by evaluating the logical and registers resources needed by the digital architecture, in particular for the hardware intercorrelation module which is the most demanding. Real tests in typical conditions (temperature, humidity) could also help validate our models for slow degradation assessments.

References

[1] Tatry, PH., F. Deneu, J.L. Simonotti. 1997. RAMS approach for reusable launch vehicle advanced studies. *Acta Astronaumica*. Volume 41, Issue 11, 791-797.
[2] Furse C., R. Haupt. 2001. Down to the Wire Tiny electrical faults occur with alarming frequency as an aircraft's wiring ages. Detecting those faults presents a daunting technical challenge. In: *IEEE SPECTRUM*. Volume 38, Issue 2, 34-41.
[3] Furse C., Y. Chung Chung, R. Dangol, M. Nielsen, G. Mabey, R. Woodward. 2003. Frequency-domain reflectometry for on-board testing of aging aircraft wiring. In: *IEEE Transactions on Electromagnetic Compatibility*. Volume 45, Issue 2, 306-315.
[4] Auzanneau F., M. Olivas, N. Ravot. 2007. A simple and accurate model for wire diagnosis using reflectometry. In: PIERS Proceedings. 232-236.
[5] Ravot N., F. Auzanneau, Y. Bonhomme, M. Olivas, F. Bouillault. 2007. Distributed reflectometry-based diagnosis for complex wired networks. In: *EMC: Safety, Reliability and Security of Communication and Transportation Systems*.
[6] Lelong. A., L. Sommervogel, N. Ravot. M. Carrion. 2009. Distributed reflectometry method for wire fault location using selective average. In: *IEEE sensors journal*. Volume 10, Issue 2. 300-310.
[7] Ben Hassen W., F. Auzanneau, F. Peres, A. Tchangani. 2012. A distributed diagnosis strategy using Bayesian network for complex wiring networks. In: *IFAC Proceedings*. Volume 45, Issue 31, 42-47.
[8] Kamel Smail M., L. Pichon, M. Olivas, F. Auzanneau. M. Lambert. 2011. Recent progress in wiring networks diagnosis for automotive applications. In: *The international journal for computation and mathematics in electrical and electronic engineering*. Volume 30. Issue 4. 1148-1161.
[9] Ben Hassen W., MG. Roman, B. Charnier, N. Ravot, A. Dupret, A. Zanchetta, F. Morel. 2016. Embedded omtr sensor for small soft fault location on aging aircraft wiring systems. In: *Procedia Engineering*. Volume 168. 1698-1701.
[10] Dumont, E., T. Ecker, C. Chavanac, L. Witte, J. Windelberg, J. Klevanski, S. Giagkozoglou. 2018. CALLISTO - Reusable VTVL launcher first stage demonstrator. In: *Space propulsion Conference 2018*. 14-18.
[11] Narula A..2012. Modeling of Ageing of Lithium-Ion Battery at Low Temperatures. Master of Science Thesis. Chalmers University of Technology, Department of Energy and Environment.
[12] Riddle, B., J. Kaker-Jarvis, J. Krupka. 2014. Complex permittivity measurements of common plastics over variable temperatures. In: *IEEE Transactions on Microwave theory and techniques*. Volume 51, issue 3. 727-733.